The effect of zirconium on the electronic structure of grain boundaries in $Ni_3Al$



1997 J. Phys.: Condens. Matter 9 4499

(http://iopscience.iop.org/0953-8984/9/22/003)

J. Phys.: Condens. Matter **9** (1997) 4499–4507. Printed in the UK PII: S0953-8984(97)75950-2

# The effect of zirconium on the electronic structure of grain boundaries in $Ni_3Al$

Wang Fuhe and Wang Chongyu

China Centre of Advanced Science and Technology (World Laboratory), Beijing 100080, People's Republic of China, and Central Iron and Steel Research Institute, Beijing 100081, People's Republic of China†

Received 4 July 1996, in final form 2 January 1997

**Abstract.** The discrete variational method within the framework of density functional theory is used to study the effect of zirconium on the electronic structure of the $\Sigma 5[001](210)$ grain boundary in $Ni_3Al$. The results for the interatomic energies show that the strength of the $Ni_3Al$ grain boundary is increased by the substitution of Zr for Al. The calculation of the charge distribution indicates that the directionality of the bonds in the grain boundary region is weakened by the addition of Zr. These results show that the alloying effect of Zr introduced into $Ni_3Al$ can significantly improve the ductility of $Ni_3Al$, while strengthening the grain boundary.

## 1. Introduction

$Ni_3Al$ has many attractive properties as a high-temperature structural material (such as high-temperature strength, low density, and resistance to oxidation). However, polycrystalline $Ni_3Al$ is a intergranularly brittle material, which is strongly affected by the 'intrinsically weak' grain boundary [1]. Studies of the effect of microalloying on the properties of materials have shown that impurities can significantly improve the ductility of polycrystalline $Ni_3Al$ [1–5]. As an interstitial element, boron was found to be the most effective in suppressing intergranular fracture, and improving the tensile ductility of $Ni_3Al$ at room temperature [1, 2]. Moreover, Takasugi and Izumi found that alloying with iron and manganese to replace aluminium significantly improves the tensile ductility, and lowers the propensity for intergranular fracture in $Ni_3Al$ [6, 7]. Recently, a study of the addition of a small amount of zirconium (0.3 at.%) also indicated an improvement in the ductility of $Ni_3Al$ [3, 8–11]; in particular, the ductility obtained in oxygen ($\sim$50%) is comparable to the highest ever ductility obtained in B-doped $Ni_3Al$ [1]. Zirconium atoms are expected to occupy the aluminium sublattice sites in $Ni_3Al$ [12–14]. Like in the case of boron in $Ni_3Al$, zirconium only increases the ductility of Ni-rich $Ni_3Al$ alloys ($\geqslant$76 at.% of Ni) [11], and the content of zirconium in $Ni_3Al$ should be controlled ($\leqslant$0.5 at.%) in order to avoid grain boundary liquation [15].

Several models have been proposed for explaining how the addition of a third element affects the ductility of $Ni_3Al$. Takasugi *et al* [6] suggested that the value of the valency difference between the third element and the constitutive solvent atom for which the third element is substituted controls the macroscopic grain boundary strength of the ternary $Ni_3Al$ intermetallic compound. When the value of the valency difference is positive, the

† Mailing address.

0953-8984/97/224499+09$19.50  

grain boundary is expected to be stronger. Taub, Briant *et al* [16, 17] used Pauling's electronegativity scale to explain the effect of boron in $Ni_3X$ (where X = Al, Ga, Si, or Ge). The valency and electronegativity models are both based on the concept that localization of electronic charge is responsible for the brittle behaviour of intermetallics. The cohesion of a grain boundary will be enhanced, and the ductility of $Ni_3Al$ will be improved, when the electronic environment of the grain boundary region is made more homogeneous by the alloying [6]. However, it is impossible to assign a single number, such as a value of the electronegativity or valency, to describe a complex phenomenon such as chemical bonding. Transition metals, in particular, may take on different valences and bonding characteristics as their environment is changed. So one must resort to quantum mechanical calculations to obtain an insight into these problems [18].

There have been many quantum mechanical calculations made to study the effect of dopants on the intergranular cohesion of transition metals [19–23] and alloys [24–27]. Eberhart and Vvedensky [24, 25] calculated the electronic states of grain boundaries in $Ni_3Al$ and $Cu_3Pd$, as well as the wave functions of crystalline $Ir_3Cr$ and $Zr_3Al$, using a multiple-scattering $X_\alpha$-method. Their results indicated that the intrinsic ductility of materials is correlated with isotropic charge distribution. Recently we calculated the electronic structure of boron-doped grain boundaries in $Ni_3Al$ by the use of the discrete variational method (DVM) with embedded-cluster models [27]. It was found that boron formed stronger bonding states with its neighbouring host atoms, and as a *bridge*, increased the cohesive strength of the grain boundaries.

The purpose of this work is to achieve an understanding of the strengthening mechanism of zirconium in the grain boundaries of $Ni_3Al$. The electronic structure of the Zr-doped grain boundary in $Ni_3Al$ is studied using the embedded-cluster DVM [28–30] within the framework of density functional theory. The method and the model are presented in section 2, the calculated results are discussed in section 3, and we give some conclusions in the last section.

## 2. The computation method and the cluster model

The discrete variational method (DVM) is a first-principles numerical method for solving the local density functional equations [28–30], and has been successfully used to study the electronic structure of metals [28], alloys [29], and grain boundaries in intermetallic compounds [27]. In this work, the DVM is used to study the electronic structure of grain boundaries in $Ni_3Al$, and the effect of zirconium. The embedded-cluster approach [29] is used, i.e., in constructing the self-consistent potential, the charge density of several hundreds of atoms surrounding the cluster in the grain boundary is included, creating an embedding potential, and thus diminishing spurious effects of simulating the solid by a cluster of atoms [28].

In the one-electron wave equation, the Hamiltonian is

$$H = -\nabla^2/2 + V_c + V_{xc} \tag{1}$$

where $V_c$ is the electron–nucleus and electron–electron Coulomb potential, and $V_{xc}$, derived by von Barth and Hedin [31], is the exchange–correlation potential. The eigenstates (or molecular orbitals) are expanded as a linear combination of the atomic orbitals $\phi_i(r)$ [28]:

$$\psi_n(r) = \sum_i C_{ni}\phi_i(r) \tag{2}$$

and the expansion coefficients $C_{ni}$ are obtained as usual by solving the secular equation

$$(H - ES)C = 0. \tag{3}$$

The Hamiltonian matrix $H$ and the overlap matrix $S$ are obtained in the discrete variational method as weighted sums over a set of sample points [28–30].

In order to study the interaction between atoms, the interatomic energy between atom $l$ and $m$ is derived [27, 32]:

$$E_{lm} = \sum_{n} \sum_{\alpha\beta} N_n a^{\star}_{n\alpha l} a_{n\beta m} H_{\beta m \alpha l} \tag{4}$$

where $N_n$ is the occupation number for the molecular orbital $\psi_n$, $a_{n\alpha l} = \langle \phi_{\alpha l}(r) | \psi_n(r) \rangle$, and $H_{\beta m \alpha l}$ is the Hamiltonian matrix element connecting the atomic orbital $\beta$ of atom $m$ and the atomic orbital $\alpha$ of atom $l$.

In the computation, the single-site orbitals are used as the basis set, and the frozen-core mode is chosen; also the funnel potential is added to induce bound excited states. The inner radius of the potential well is set at 4 au, with the potential-well depth and the cut-off radius being $-2.0$ and 6.0 au, respectively. The non-spin-polarized secular equations are solved using the self-consistent-charge (SCC) approximation.

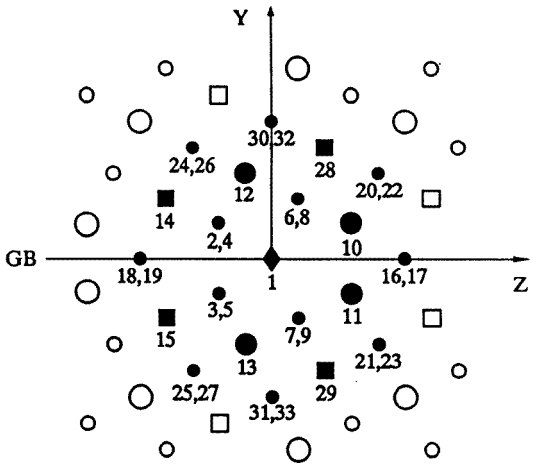


**Figure 1.** The atomic configurations around the $\Sigma 5[001](210)$ tilt grain boundaries in $Ni_3Al$. The Ni and Al atoms are represented by the circles and squares, the different sizes represent different layers, and the atoms shown as large symbols are in the $YZ$-plane. The atoms shown as solid symbols and labelled by numbers are in the cluster, and the solid diamond represents the site of substitution of Zr for $Al_1$.

The grain boundary $\Sigma 5[001](210)$, which is constructed by use of the coincidence-site lattice model [33] and atomistic simulations [34], is investigated. Figure 1 shows the atomic configuration for the $\Sigma 5$ grain boundary in $Ni_3Al$. The cluster atoms shown as solid symbols (in figure 1) are embedded in 348 surrounding atoms. In order to clarify the discussion of the interaction between atoms, the atoms in the cluster are labelled with numbers. With a method like that of Masuda-Jindo [35], the atomic relaxation is carried out by the energy-minimization procedure in which a proportion of the atoms at a grain boundary are pulled apart from the interface. When the minimum of binding energy is achieved for the cluster system, the equilibrium configuration is given.

**Table 1.** The interatomic energies (in eV) of the adjacent atoms in the Zr-doped ($E_{GB+Zr}$) and clean ($E_{GB}$) grain boundaries; $\Delta E = E_{GB+Zr} - E_{GB}$ is the change of interatomic energy induced by the substitution of Zr for an $Al_1$ atom, and $E_{bulk}$ is the interatomic energy for the nearest-neighbouring atoms in the bulk $Ni_3Al$.

| Pairs of atoms | $Al_1$ (Zr)–$Ni_2$ | $Al_1$ (Zr)–$Ni_6$ | $Al_1$ (Zr)–$Ni_{10}$ | $Al_1$ (Zr)–$Ni_{12}$ | $Ni_2$–$Ni_3$ | $Ni_6$–$Ni_7$ | $Ni_{10}$–$Ni_{11}$ |
|---|---|---|---|---|---|---|---|
| $E_{GB}$ | −1.437 | −1.406 | −1.465 | −0.997 | −3.829 | −0.559 | −2.504 |
| $E_{GB+Zr}$ | −1.833 | −1.807 | −1.874 | −1.423 | −4.037 | −0.650 | −2.634 |
| $\Delta E$ | −0.396 | −0.401 | −0.409 | −0.426 | −0.208 | −0.091 | −0.130 |
| $E_{bulk}$ | $E_{Ni-Al} = -1.536$ | | | | $E_{Ni-Ni} = -1.755$ | | |

## 3. Results and discussion

### *3.1. Interatomic energy*

The interatomic energies defined by equation (4) are calculated for Σ5 grain boundaries without and with Zr, and the results are listed in table 1. In order to show the effect of zirconium clearly, the changes induced by the substitution of Zr for Al are presented. The interatomic energies for the nearest-neighbouring (NN) atoms in bulk $Ni_3Al$ are calculated using an embedded cluster containing 43 atoms, and the results are listed in table 1 too. From table 1 it can be found that the interatomic energies for the atoms at the grain boundary are enhanced when an $Al_1$ atom is replaced by Zr. In particular, the interatomic energies for Zr and its adjacent atoms are strongly enhanced relative to the interatomic energies for $Al_1$ and corresponding atoms. As a result, it can be predicted that the strength of the grain boundary in $Ni_3Al$ is increased by the substitution of Zr for Al, and this can be used to explain the experimental phenomena for $Ni_3Al$-doped Zr [8–11].

The interatomic energies for the Al–Ni pairs in the clean grain boundary are higher than those in the bulk (comparing those pairs of atoms which have the almost same interatomic distance as in the bulk, such as $Al_1$–$Ni_2$, $Al_1$–$Ni_6$, $Al_1$–$Ni_{10}$, and $Al_1$–$Ni_{12}$). Considering the broken symmetry of the grain boundary and the fact that some micro-voids existed in the region near the grain boundary, the charge distributions near the grain boundary are not as homogeneous as in the bulk of $Ni_3Al$. As a result, the cohesion of the grain boundary will be weakened, and the fracture mode can be changed into an intergranular-type mode in polycrystalline $Ni_3Al$. When Zr is added to substitute for Al, the interatomic energies for Zr and its adjacent atoms become lower than that for the Ni–Al pairs in the bulk $Ni_3Al$, and so the strength of the grain boundary is increased, especially in the region near to Zr. It can be understood that the ultimate tensile strength of Zr-doped polycrystalline $Ni_3Al$ (661 MPa in air and 1451 MPa in oxygen [8, 11]) is much larger than that of clean polycrystalline $Ni_3Al$ (392 MPa in air [4]).

### *3.2. Charge distribution*

The electron density difference is obtained by subtracting the electron density of the clean grain boundary from that of the Zr-doped grain boundary, and the electron density difference between free Zr and the free Al atom is also deducted, i.e., $\Delta\rho = \rho(\mathrm{GB} + \mathrm{Zr}) - \rho(\mathrm{GB}) - (\rho_{free}(\mathrm{Zr}) - \rho_{free}(\mathrm{Al}))$. To show the Zr-induced charge redistribution more clearly [21], in figure 2 we have given the electron density difference plotted in different planes.

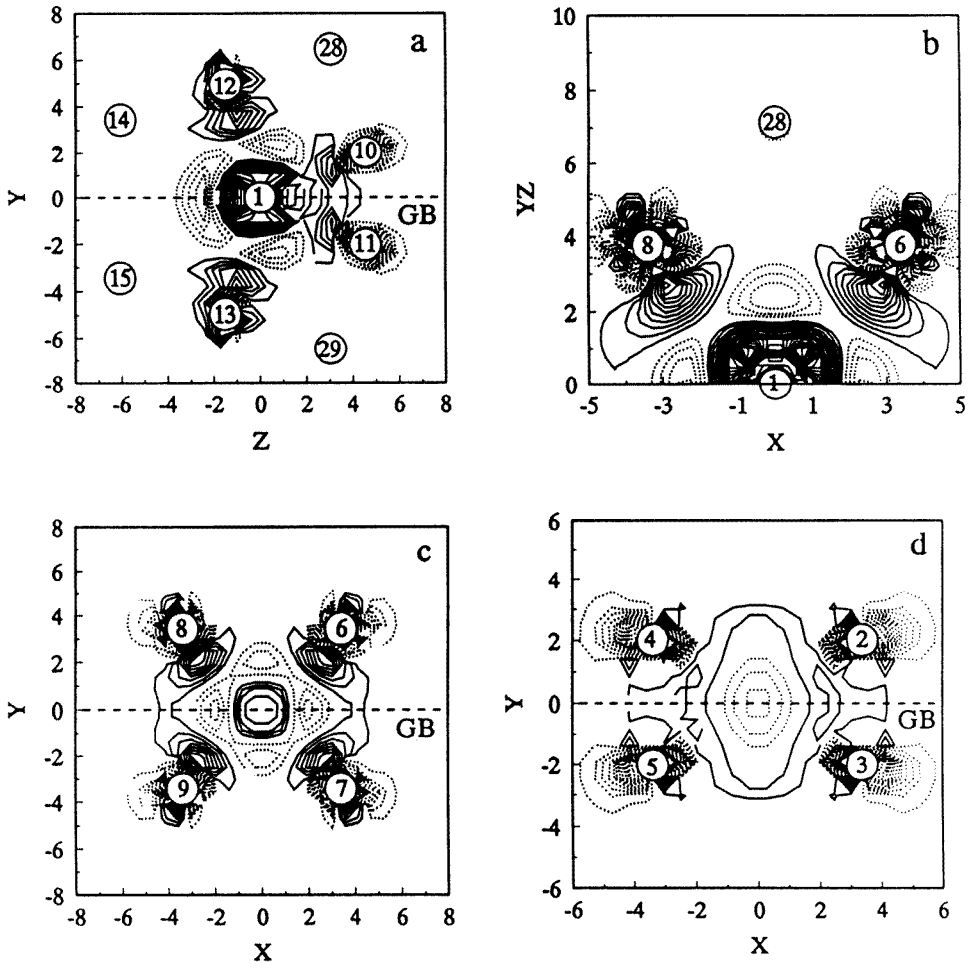


**Figure 2.** The electron density difference between a Zr-doped grain boundary and a clean grain boundary for different planes: (a) the $YZ$-plane; (b) the plane containing $Al_1$ (Zr), $Ni_6$, $Ni_8$, and $Al_{28}$ atoms; (c) the plane containing $Ni_6$, $Ni_7$, $Ni_8$, and $Ni_9$ atoms; and (d) the plane containing $Ni_2$, $Ni_3$, $Ni_4$, and $Ni_5$ atoms. The circled numbers, which correspond to those in figure 1, indicate the positioning of atoms in the plane. The contour spacings are $0.001e$ au$^{-3}$. Solid lines indicate the gain of an electron, and dashed lines indicate the loss of an electron.

It can be seen that the electron density in the intermediate region between atom No 1 (Zr or $Al_1$) and its neighbouring atoms is distinctly increased by the substitution of Zr for Al, so the bonding for Zr and its neighbouring atoms is stronger than that for $Al_1$ and its neighbouring atoms when $Al_1$ is replaced by Zr. From figures 2(c) and 2(d), it can be found that the electron density between host atoms, such as $Ni_2$–$Ni_3$ and $Ni_6$–$Ni_7$, which are situated on the other side of the grain boundary, is also increased by the substitution of Zr for $Al_1$. Therefore, the bonding strength for host atoms which are near to the substitution site is increased by the substitution. These calculated results are consistent with the results for interatomic energies given in section 3.1.

The electron occupation number $N$ in valence orbitals is calculated by the use of Mulliken analysis. The net number of electrons $Q = N - Z_{\mathrm{val}}$ ($Z_{\mathrm{val}}$ is the standard number

**Table 2.** The electron occupation number $N$ in the valence orbitals, and the net number of electrons $Q = N - Z_{val}$ for each atom, the changes $\Delta N = N_{GB+Zr} - N_{GB}$ and $\Delta Q = Q_{GB+Zr} - Q_{GB}$ induced by the substitution of Zr for $Al_1$.

| | | $N_{GB}$ | $N_{GB+Zr}$ | $\Delta N$ | $\Delta Q$ |
|---|---|---|---|---|---|
| $Al_1$ (Zr) | 3(5)s | 1.182 | 0.343 | — | |
| | 3(5)p | 1.549 | 0.393 | — | |
| | (4)d | | 2.567 | — | |
| | $Q$ | −0.269 | −0.697 | | −0.428 |
| $Ni_2$ | 4s | 0.937 | 0.947 | 0.010 | |
| | 4p | 0.875 | 0.896 | 0.021 | |
| | 3d | 8.254 | 8.260 | 0.006 | |
| | $Q$ | 0.066 | 0.103 | | 0.037 |
| $Ni_6$ | 4s | 0.929 | 0.964 | 0.035 | |
| | 4p | 0.786 | 0.817 | 0.031 | |
| | 3d | 8.282 | 8.277 | −0.005 | |
| | $Q$ | −0.003 | 0.058 | | 0.061 |
| $Ni_{10}$ | 4s | 0.828 | 0.857 | 0.029 | |
| | 4p | 0.758 | 0.786 | 0.028 | |
| | 3d | 8.306 | 8.304 | −0.002 | |
| | $Q$ | −0.108 | −0.053 | | 0.055 |
| $Ni_{12}$ | 4s | 0.786 | 0.812 | 0.026 | |
| | 4p | 0.757 | 0.785 | 0.028 | |
| | 3d | 8.293 | 8.293 | 0.000 | |
| | $Q$ | −0.164 | −0.110 | | 0.054 |

of valence electrons per atom) for each atom is also calculated. The results are presented in table 2. From the calculated results, it can be seen that $Al_1$ loses the electrons for the clean grain boundary, and Zr loses more electrons for the Zr-doped grain boundary. This is consistent with the fact that Pauling's electronegativity for Zr is the smallest among these elements (Pauling's electronegativities for these elements are 1.33 for Zr, 1.61 for Al, and 1.91 for Ni [36]). A free Zr atom has two electrons in each of the 5s and 4d orbitals. When Al is replaced by Zr, there is one additional electron in the system. Referred to the free Zr atom, a proportion of the electrons in the 5s orbital are transferred to the 4d (0.567 electrons) and 5p (0.393 electrons), and 0.697 electrons are lost. From table 2, it can also be found that the numbers of electrons in the s and p orbitals of host atoms are increased, but the number of electrons in d orbitals is hardly changed when $Al_1$ is replaced by Zr. This indicates that the electrons lost from Zr are mainly shared by the s and p orbitals of neighbouring atoms. This may indicate a reduction in the directionality of the bonds in the Zr-doped grain boundary relative to that in the clean grain boundary, because of the dispersed distribution in space of s and p electrons. Furthermore, the total numbers of valence electrons for each host atom which is near to a substitution site is increased by the addition of Zr. This shows that electrons can be shared between atoms as in ductile metals [18].

### *3.3. Density of states*

The densities of states (DOS) are obtained by broadening the discrete eigenvalue spectrum with a set of Lorentzian functions [28]. The partial densities of states (PDOS) of some

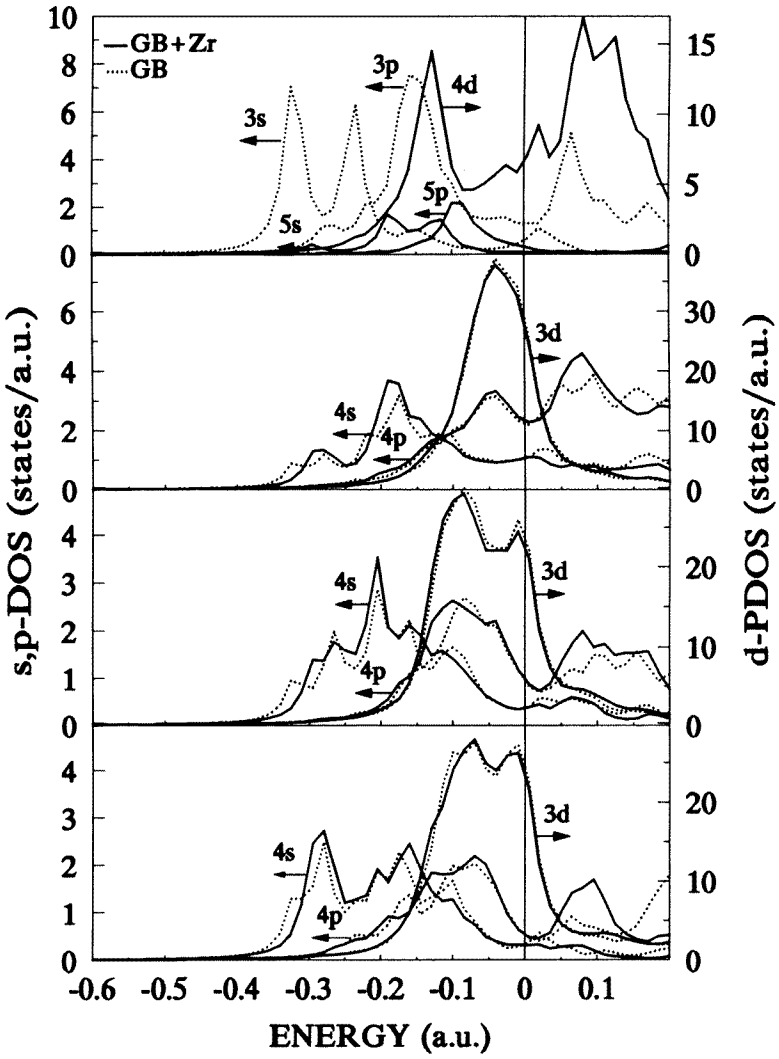


**Figure 3.** The partial density of states (PDOS) of $Al_1$ (Zr) and its neighbouring atoms in the $Ni_3Al$ grain boundary. The solid and dotted lines represent the PDOS of the atoms in the doped and clean grain boundaries respectively.

atoms are shown in figure 3. Comparing the PDOS of Zr with that of $Al_1$, it can be seen that the main peaks of the s and p PDOS of Zr are located in the region of higher energy (in which the main peaks of the PDOS of Ni are located too) relative to that of $Al_1$. As a result, the hybridization between Zr and its neighbouring atoms is stronger than that for $Al_1$ and the corresponding atoms, especially as regards the hybridization between Zr p and Ni d partial waves. It should be noted that the d electrons of Zr bear the predominant responsibility for the bonding between the Zr atom and its adjacent atoms; in contrast, the Al atom has no d electrons. The d electrons of Zr hybridize strongly with the s, p, d electrons of its adjacent Ni atoms, and this makes the interaction between Zr and its neighbouring atoms very strong. This is in agreement with the calculated results for the interatomic energy.

Another feature of the change of the DOS is that the magnitude of the d PDOS of Ni at the Fermi level is slightly reduced when $Al_1$ is replaced by Zr. The reduction of the DOS near the Fermi level means that the transition probability of the electronic states is confined, and the stability of the grain boundary is increased [27]. This is similar to the effect of B in the $Ni_3Al$ grain boundary [27, 37].

## 4. Conclusion

We have studied the effect of Zr on the electronic structure of the grain boundary in $Ni_3Al$ using first-principles numerical calculations. It is found that the strength of the bonding between Zr and its neighbouring atoms in a Zr-doped grain boundary is higher than that for $Al_1$ and the corresponding atoms in a clean grain boundary. Moreover, the bonds between host atoms are also strengthened by the substitution of zirconium for aluminium. On the other hand, the directionality of the bonds in the region of the grain boundary is weakened when a proportion of the Al atoms are replaced by Zr. This will enhance the cohesive strength, and probably make movement of dislocations easier at the grain boundary in $Ni_3Al$. It can be concluded that the alloying of Zr into $Ni_3Al$ can strengthen the cohesion of the grain boundary.

## Acknowledgments

We are grateful to Professor J M Li and Dr J L Yang for beneficial discussions. This work was supported by the National Natural Science Foundation of China.

## References

[1] Liu C T, White C L and Horton J A 1985 *Acta Metall.* **33** 213
[2] Aoki K and Izumi O 1979 *J. Japan Inst. Met.* **43** 1190
[3] Aoki K 1990 *Mater. Trans. Japan Inst. Met.* **31** 443
[4] Liu C T 1993 *Structural Intermetallics* ed R Darolia, J J Lewandowski, C T Liu, P L Martin, D B Miracle and M V Nathal (Warrendale, PA: The Minerals, Metals and Materials Society) p 365
[5] Chiba A, Hanada S and Watanabe S 1992 *Mater. Sci. Eng.* A **152** 108
[6] Takasugi T, Izumi O and Masahashi N 1985 *Acta Metall.* **33** 1259
[7] Izumi O 1989 *Mater. Trans. Japan Inst. Met.* **30** 627
[8] George E P, Liu C T and Pope D P 1992 *Scr. Metall.* **27** 365
[9] George E P, Liu C T and Pope D P 1993 *Mater. Res. Soc. Symp. Proc.* **288** 941
[10] George E P, Liu C T and Pope D P 1993 *Scr. Metall.* **28** 857
[11] George E P, Liu C T and Pope D P 1993 *Structural Intermetallics* ed R Darolia, J J Lewandowski, C T Liu, P L Martin, D B Miracle and M V Nathal (Warrendale, PA: The Minerals, Metals and Materials Society) p 431
[12] Ochiai S, Oya Y and Suzuki T 1984 *Acta Metall.* **32** 289
[13] Machlin E S and Shao J 1977 *Scr. Metall.* **11** 859
[14] Sluiter M H F and Kawazoe Y 1995 *Phys. Rev.* B **51** 4062
[15] Chen G H and Chen C 1992 *Scr. Metall.* **27** 121
[16] Taub A I, Briant C L, Huang S-C, Chang K-M and Jackson M R 1986 *Scr. Metall.* **20** 129
[17] Taub A I and Briant C L 1987 *Acta Metall.* **35** 1597
[18] Briant C L 1994 *Intermetallic Compounds: 1, Principles* ed J H Westbrook and R C Fleischer (New York: Wiley) p 895
[19] Messmer R P and Briant C L 1982 *Acta Metall.* **30** 457
[20] Painter G S and Averill F W 1987 *Phys. Rev. Lett.* **58** 234
[21] Tang S, Freeman A J and Olson G B 1994 *Phys. Rev.* B **50** 1
[22] Wu R, Freeman A J and Olson G B 1994 *Phys. Rev.* B **50** 75
[23] Krasko G L 1994 *Mater. Res. Soc. Symp. Proc.* **319** 369

[24] Eberhart M E and Vvedensky D D 1987 *Phys. Rev. Lett.* **58** 61
[25] Eberhart M E and Vvedensky D D 1988 *Phys. Rev.* B **37** 8488
[26] Masuda-Jindo K 1995 *Mater. Sci. Eng.* A **192+193** 104
[27] Wang F H, Wang C Y and Yang J L 1996 *J. Phys.: Condens. Matter* **8** 5527
[28] Guenzburger D and Ellis D E 1992 *Phys. Rev.* B **46** 285
[29] Ellis D E, Benesh G A and Bykom E 1977 *Phys. Rev.* B **16** 3308
[30] Delley B, Ellis D E, Freeman A J, Baerends E J and Post D 1983 *Phys. Rev.* B **27** 2132
[31] von Barth U and Hedin L 1972 *J. Phys. C: Solid State Phys.* **5** 1629
[32] Wang C Y, Dou C Y, Zeng Y P, Gao L and Liu F S 1989 *Proc. Int. Workshop on the Physics of Materials (Shenyang)* abstracts, p B5-1
[33] Takasugi T and Izumi O 1983 *Acta Metall.* **31** 1187
[34] Chen S P, Voter A F and Srolovitz D J 1986 *Scr. Metall.* **20** 1389
[35] Masuda-Jindo K 1982 *J. Physique* **43** 921
[36] Heslop R B and Jones K 1976 *Inorganic Chemistry* (Amsterdam: Elsevier)
[37] Muller D A, Subramanian S, Batson P E, Sass S L and Silcox J 1995 *Phys. Rev. Lett.* **75** 4744